Response of the climatic mass balance of Hurd and Johnsons glaciers, Livingston Island, to the transient cooling period of the northern Antarctic Peninsula in the early 21st century

Cayetana Recio-Blitz[1,2], María Isabel de Corcuera[3], Francisco Machío[4], Ricardo Rodríguez-Cielos[5], Francisco Navarro[3*]

[1]*Facultad de Ciencias Sociales y Humanidades, Universidad Isabel I, Calle Fernán González 76, 09003 Burgos, Spain*
[2]*Facultad de Educación, Universidad Camilo José Cela, Calle Castillo de Alarcón 49, 28692 Villafranca del Castillo, Madrid, Spain*
[3]*Departmento de Matemática Aplicada a las TIC, ETSI de Telecomunicación, Universidad Politécnica de Madrid, Av. Complutense, 30, 28040 Madrid, Spain*
[4]*Escuela Superior de Ingeniería y Tecnología, Universidad Internacional de La Rioja, Avenida de la Paz 137, 26006 Logroño, Spain*
[5]*Departmento de Señales, Sistemas y Radiocomunicaciones, ETSI de Telecomunicación, Universidad Politécnica de Madrid, Av. Complutense 30, 28040 Madrid, Spain*

Abstract

We calculated and analysed the climatic mass balance of Hurd and Johnsons glaciers, Livingston Island, northern Antarctic Peninsula region, over the period 2002−2016. This period is nearly coincident with the transient period of sustained cooling occurred in the northern Antarctic Peninsula region in the early 21st century. A positive trend for the climatic mass balance of ~0.5-0.6 m w.e. decade^{-1} was observed, in parallel with a striking negative trend of the equilibrium line altitude of ~ −100-200 m decade^{-1}, and a positive trend of the accumulation area ratio of ~3-6% decade^{-1}. Other glaciers monitored in the South Shetland Islands and the periphery of the northernmost Antarctic Peninsula have shown a similar behavior, with the changes observed in the former being more marked.

Key words: Accumulation, ablation, Hurd Peninsula, South Shetland Islands

DOI: 10.5817/CPR2023-2-19

***List of abbreviations*:** AAR − Accumulation Area Ratio, AP − Antarctic Peninsula, CMB − Climatic Mass Balance, DEM − Digital Elevation model, ELA − Equilibrium Line Altitude, GNSS − Global Navigation Satellite System, GTN-G − Global Terrestrial Network for Glaciers, IPCC − Intergovernmental Panel on Climate Change, JCI − Juan Carlos I (Spanish Antarctic research station), w.e. − water equivalent, RMSE − Root-Mean Square Error, SLR − Sea-Level Rise, WGMS − World Glacier Monitoring Service

Received December 19, 2023, *accepted* January 22, 2024.
*Corresponding author: F. Navarro <francisco.navarro@upm.es>
Acknowledgements: This research was funded by grants CTM2017-84441-R and PID2020-113051RB-C31 from MCIN/AEI/10.13039/501100011033/FEDER, UE.

Introduction

Mass losses from glaciers and ice sheets are currently contributing to about 45% of the observed sea-level rise (SLR), of 3.7 mm a^{-1} for the period 2006–2018 (Fox-Kemper et al. 2021, IPCC 2022). The more than 200 000 glaciers distributed across the globe (Pfeffer et al. 2014), which only comprise ca. 1% of the total landed ice volume, contribute to current SLR almost as much as the large ices sheets of Antarctica and Greenland, which store roughly 11% and 88% of the total landed ice volume (Navarro 2021). The reason for the comparatively huge contribution of glaciers is their small size compared to the large ice sheets, which makes glaciers especially sensitive, and with much faster response time, to climate change.

The Antarctic periphery holds many glaciers disconnected from the main ice sheet, most of them located on islands surrounding the continent. These glaciers form the so-called Region 19-Antarctic and Subantarctic of the Glacier Regions classification of the Global Terrestrial Network for Glaciers (GTN-G)[1]. 63% (by area) of such glaciers are located in the islands surrounding the Antarctic Peninsula (AP), a region that has experienced an atypical climate evolution in recent decades. During the second half of the 20th century, the AP region experienced one of the strongest warming trends on Earth, of 0.57 ± 0.2°C per decade during 1951–2001 as recorded in Faraday/Vernadsky station (Vaughan et al. 2003). A relatively short but sustained cooling period followed, spanning between the end of the 20th century and the mid-2010s (Turner et al. 2016). This cooling mostly focused on the northern AP and the South Shetland Islands (SSI) (Oliva et al. 2017), where winter (summer) temperature decreased in the order of 1.0°C (0.5°C) per decade between the decades 1996–2005 and 2006–2015. Afterwards, a return to warming conditions has been observed (Carrasco et al. 2021). In parallel, multi-decadal increases in snowfall have been inferred since the 1930s (Medley and Thomas 2019). These temperature and snow precipitation changes have implied fluctuations of the climatic mass balance (CMB) of the glaciers in this region. Although the current contribution to SLR of the glaciers in the Antarctic periphery is small (Zemp et al. 2019, Hugonnet et al. 2021), it is projected to increase substantially to the end of the 21st century (Edwards et al. 2021), and hence the interest of their study.

The aim of this paper was to analyse the impact of the recent cooling period on the climatic mass balance of the glaciers on the South Shetland Islands, on the basis of the study of two glaciers, Hurd and Johnsons, located on Livingston Island. The evolution of the climatic mass balance of such glaciers was studied by Navarro et al. (2013) for the 10-year period 2002–2011. Here we expand such CMB series to the period 2002–2016, to cover the entire duration of the cooling period. Moreover, we recomputed the CMB of the whole time series by using an updated glacier geometry (glacier outlines and surface elevations) for each individual year. Hurd and Johnsons glaciers are specially relevant in the context of regional mass balance studies, as they are two of the three only glaciers that currently have climatic mass balance series longer than 20 years in the database of the World Glacier Monitoring Service (WGMS)[2] for Region 19-Antarctic and Subantarctic.

Geographical setting

Hurd and Johnsons glaciers are the two main units of the ice cap covering the Hurd Peninsula (62° 39' – 62° 42' S, 60° 19' – 60° 25' W), in Livingston Island, the sec-

ond largest of the South Shetland Islands, to the North of the AP (Fig. 1). These glaciers span an altitude range from 0 to 370 m a.s.l. Hurd Glacier (4.03 km^2) is a land-terminating glacier flowing mostly to the southwest. It has three major lobes: Argentina, Las Palmas and Sally Rocks. Johnsons Glacier (5.36 km^2), in turn, is a tidewater glacier (a sea-terminating glacier with terminus grounded below sea level), which flows mostly to the northwest and ends on an ice cliff of 50 m in height extending 500-600 m along the coast. Both glaciers are separated by an ice divide with altitudes between 250 and 330 m a.s.l. Hurd Glacier has an average surface slope of approximately 3°, although its western-flowing lobes, Argentina and Las Palmas, have much steeper slopes, ca. 13°. Typical slopes of Johnsons Glacier range between 6° in the south and 10° in the north; the slopes become more gentle as the calving front is approached, except at sections of the front where it locally collapses. Being a tidewater glacier, Johnsons has ice surface velocities substantially larger than those of the land-terminating Hurd Glacier. For Johnsons, the velocities increase towards the calving front, where values up to 65 m a^{-1} are attained (Otero et al. 2010, Machío et al. 2017). By contrast, the highest ice velocities for Hurd Glacier are just about 5 m a^{-1} and are reached at its central basin, decreasing towards the frozen-to-bed terminal zones (Machío et al. 2017).

Hurd glacier has a Scandinavian-type polythermal structure, with a top layer of cold ice, several tens of metres thick, on the ablation zone (Letamendia et al. 2023), while the polythermal structure of Johnsons Glacier is more irregular, with irregularly-distributed patches of cold ice (Navarro et al. 2009, Sugiyama et al. 2019).

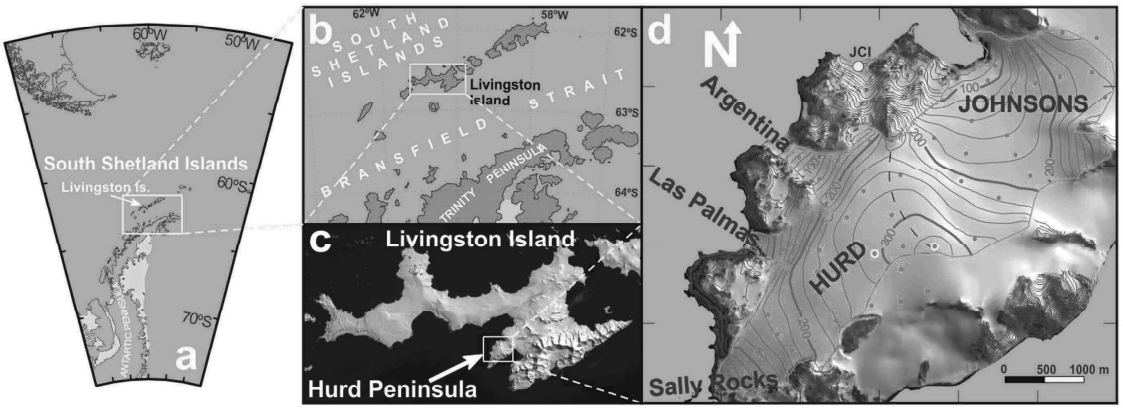

Fig. 1. Location of the South Shetland Islands archipelago (a), Livingston Island (b) and Hurd Peninsula (c); background image is a Copernicus Sentinel image of 2013. The map in panel d represents the surface elevation of Hurd and Johnsons glaciers and the location of the mass balance stakes in the hydrological year 2016 (red dots), of the three snow pits with most abundant data (yellow-circled red dots) and of Juan Carlos I Station (JCI, yellow dot). The continuous blue line represents the glacier outlines and the dashed blue line indicates the ice divide separating Hurd and Johnsons glaciers. The glacierized zone on the southeast of Hurd Peninsula without contour lines corresponds to other glacier basins, flowing to the southeast, which are not addressed by this study. Four of the stakes shown in the figure are located in this zone, and thus outside of our study area. We kept them in the figure because their values were used to interpolate (rather than extrapolate) the SMB values of Hurd Glacier in this zone. The area shown in panel d corresponds to the UTM coordinates 631000-637000 (easting) and 3045000-3050000 (northing) for UTM sheet 20E. The separation between tick marks represents a distance of 1 km.

Hurd Peninsula shows the typical maritime climate of the western coast of the Antarctic Peninsula. The mean annual temperature at the Spanish Antarctic Station Juan Carlos I (JCI in Fig. 1) over the period 1994−2014 was -1.2°C, with mean summer (December-January-February) and winter (June-July-August) temperatures of 1.9 and -4.7°C, respectively (Bañón and Vasallo 2015).

Material and Methods

A note on terminology

We follow in this paper the mass balance terminology, symbols and units recommended by Cogley et al. (2011).

Glacier mass gains are termed as accumulation, while mass losses are termed as ablation. The surface mass balance is the sum of surface accumulation and surface ablation, *i.e.* the net result of mass gains and losses taking place at the glacier surface. This is the normal use of this term in descriptions of measurements by the glaciological method, in which the internal mass balance is treated separately. However, as pointed out by Cogley et al. (2011), an ambiguity arises because, in estimates of ice-sheet mass balance by modelling starting roughly in the early 2000s, the meaning of surface mass balance was extended to also include internal accumulation. To avoid confusion it is preferable to avoid the latter usage, and use instead the term climatic mass balance (CMB) for the sum of the surface mass balance and the internal mass balance. The qualifier "climatic" is motivated by the fact that the surface and internal balances both depend strongly on the interactions between glacier, hydrosphere and atmosphere.

The part of the glacier where the annual surface mass balance is positive is called accumulation zone, while that where it is negative is termed as ablation zone. The line separating both zones (*i.e.* where the surface mass balance is zero) is the equilibrium line. The quotient of the area of the accumulation zone to the total area of the glacier is called the accumulation area ratio (AAR).

Following Cogley et al. (2011), we use b and B to denote mass balance, with the lower-case symbol meaning its value at a given point on the glacier surface or the column beneath such a point, and the upper-case symbol meaning the glacier-wide quantity. The subscripts w, s and a are used for representing winter, summer and annual values. The mass balance years used throughout this paper are hydrological years for the Southern Hemisphere, so year 2002 starts 1 April 2001 and ends 31 March 2002. Therefore, when we refer to the mass balance observation period 2002−2016 we mean the period from 1 April 2001 to 31 March 2016.

Field data

We use accumulation and ablation data taken from stake readings and snow probing, as well as snow density measured in snow pits. The stake readings are taken at a network of stakes deployed by the authors on Johnsons and Hurd glaciers in 2000 − 2001. It comprises about 50 stakes, distributed as homogeneously as possible across the accumulation an ablation zones (Fig. 1). The stakes are measured twice per year, at the beginning and at the end of the austral summer season, close to the yearly opening and closing of JCI station, which operates only during the austral summer. The stake measurements include the length of stake above the snow/ice surface (or

below, if buried under the winter snowpack) and, if the stakes are not in vertical position, their tilt and the orientation of tilt. The snow depth around the stake is also measured by snow probing. Differential GNSS (Global Navigation Satellite System) measurement of the stakes is also performed for positioning purposes and to calculate the summer, winter and annual mean ice velocities by calculating changes in positioning over the time period between measurements. The snow depth at the stake locations is complemented by additional snow probing at other ca. 50 locations (not shown in Fig. 1) homogeneously distributed between the whole set of stakes.

Since the 2003–2004 campaign we also perform on a regular basis snow density versus depth measurements at snow pits. As the stake readings, these measurements are carried out twice per year, at the beginning and the end of the melting season. Snow pits are currently dug at five locations in the accumulation zone of our study glaciers, though only three of the pits have data covering the period 2004–2016 (its location is marked in Fig. 1). The pits are dug to the depth of the previous summer surface, which is typically close to 2 m at the end of the winter season. Density measurements are taken at ca. 0.2 m in depth intervals, with an estimated accuracy of 10 kg m^{-3}. This provides density-versus-depth functions $\rho_w^k(H)$ and $\rho_s^k(H)$ for the end-of-winter and end-of-summer snowpacks of year k, which are used, together with the stake readings, to calculate the climatic mass balance as described below.

Climatic mass balance calculation

The CMB is calculated by the glaciological method, as described in Cogley et al. (2011). Using the accumulation and ablation data from the stake network, the snow thickness data from snow probing and the density data from the snow pits, we calculate point CMBs for winter, summer, and entire years. The density-versus-depth function $\rho_w^k(H)$ and the snow depth of the end-of-winter snowpack are used to calculate the point winter balance b_w (expressed in m in water equivalent, m w.e.). The function $\rho_s^k(H)$ and the snow depth of the end-of-summer snowpack are used, together with the ice density (for which we assume 900 kg m^{-3}), to calculate the point summer balance b_s. The ice density is used for the points in the ablation zone, where all of the winter snowpack is melted away during the summer, and also some ice down to a certain depth is melted. From these data, the point annual balance b_a is calculated as $b_a = b_w + b_s$ (with b_s a negative quantity, as it represents mass losses). Because JCI station only operates during the summer season, the last set of glacier measurements is normally carried out with some advance to the actual end of the melting season. We therefore apply a correction to b_s to account for the melting occurred after the closing of JCI station. This correction is quantified as the discrepancy between the stake readings the end of a given field season and that from the first measurement of the subsequent field season. From the whole set of calculated point CMBs, glacier-wide winter (B_w), summer (B_s) and annual (B_a) CMBs are calculated by interpolation and integration over the entire glacier, using a digital elevation model (DEM) with 25-m grid cells and a kriging routine. The accumulation area ratio, AAR, is calculated as the ratio of 25-m grid cells with b_a exceeding zero to the total number of cells. The equilibrium line altitude, ELA, is calculated, considering elevation bands of 5 m, as the band with b_a closest to zero. Additional details can be found in Navarro et al. (2013). The estimated accuracy of the calculated CMBs is between ±0.1 (Jansson 1999) and ±0.2 m w.e. (Dyurgerov 2002).

Updated glacier geometry

The ice divides used by Navarro et al. (2013) were based on manual delineation from a DEM of Johnsons-Hurd glaciers available for 2000 that is described in Molina et al. (2007). To better resolve the ice divides, in the Antarctic campaign 2012–2013 differential GNSS measurements were carried out at both sides of each divide to determine more accurately the line of change in the direction of the slope. These updated divides were used in later studies such as Rodríguez-Cielos et al. (2016). More recently, we built a DEM for Hurd Peninsula based on TanDEM-X and TerraSAR-X acquisitions on 04/08/2014 (ascending orbit number 39585, with incidence angle of ~38.5° and ambiguity height of ~166 m). ASTER GDEM v1[3] was used as reference DEM. The final DEM produced from TanDEM-X data had a horizontal resolution of 12 m. Although, when validated against differential GNSS height measurements on snow/ice-free terrain, the root-mean square error (RMSE) of the global TanDEM-X DEM is < 1.4 m (Wessel et al. 2018), over glacierized terrain the accuracy of the global TanDEM-X DEM decreases to 6.37 m when compared with ICESat data (Rizzoli et al. 2017). For Livingston Island, the latter comparison provided similar results of 6.33 m (Recio-Blitz 2019). From the TanDEM-X DEM for Hurd Peninsula, we calculated de the ice divides by means of programs for delimitation of hydrological catchments such as Catchment area (Terrain Analysis-Hydrology), from SAGA GIS[4], and r.flow, from GRASS GIS[5]. Additionally, we employed some of the *in situ* differential GNSS measurements done during the Antarctic campaign 2012–2013 to resolve some uncertainties in the delineation of the divides.

The changing position of the glacier terminus for the land-terminating lobes of Hurd glacier (Argentina, Las Palmas and Sally Rocks) was determined from differential GNSS measurements carried out at the end of the summer season for 7 out of the 15 years covered by this study. For those years without an available front position measurement, the position was linearly interpolated from the preceding and subsequent measurements. For the sea-terminating Johnsons Glacier, there were available calving front position measurements from terrestrial photogrammetry for three years, and from photogrammetric restitution of aerial photographs for two additional years. The calving front position for intermediate years was determined by linear interpolation. Further details can be found in Rodríguez-Cielos et al. (2016) and Recio-Blitz (2019).

Using the detailed DEMs available for December 2000 and February 2013, constructed from surface-based classical topography (theodolite plus laser distance ranger) (Molina et al. 2007) and differential GNSS measurements (Rodríguez-Cielos 2014), together with the updated ice divides and glacier terminus positions described above, a DEM for each individual year within our study period 2002–2016 was built following the procedure described by Mensah et al. (2022). Extrapolation was needed in the case of the DEMs for 2014, 2015, 2016, which are therefore expected to have decreasing accuracies.

Results

The glacier-wide winter, summer and annual climatic mass balances (B_w, B_s and B_a, respectively), the ELA and the AAR for each glacier and hydrological year with-

in the period 2002–2016 are shown in Table 1.

From the table we observe that, while Hurd Glacier shows an average climatic mass balance close to equilibrium (-0.04 m w.e.), Johnsons shows a positive balance (0.21 m w.e.), with higher interannual variability for Hurd than for Johnsons (as illustrated by their corresponding standard deviations). For both glaciers, the interannual variability of the summer balance is larger than that of the winter balance, with the difference more marked in the case of Hurd. While the summer average balances are quite similar for both glaciers, the winter balance of Johnsons is clearly larger than that of Hurd. We attribute this to the prevailing southern winds at the ice divide separating both glaciers and the concave shape of Johnsons Glacier, as compared with the convex (ice-cap-like) shape of the upper elevations of Hurd Glacier, implying that part of the snow originally deposited on the upper reaches of Hurd Glacier is blown by wind and deposited on Johnsons Glacier. The average ELA is lower, and the AAR is larger for Johnsons as compared with Hurd, which is consistent with the hypsometry (distribution of glacier area versus elevation) of both glaciers, shown in Fig. 2, which illustrates that Johnsons as a larger share of area at lower elevations.

	Hurd Glacier					Johnsons Glacier					
Hydrol. Year	Bw (m w.e.)	Bs (m w.e.)	Ba (m w.e.)	ELA (m)	AAR (%)	Hydrol. Year	Bw (m w.e.)	Bs (m w.e.)	Ba (m w.e.)	ELA (m)	AAR (%)
2002	0.53	-0.77	-0.25	245	35	2002	0.72	-0.69	0.04	175	64
2003	0.54	-0.97	-0.42	305	15	2003	0.69	-0.79	-0.10	185	55
2004	0.63	-0.67	-0.04	245	39	2004	0.70	-0.62	0.08	165	69
2005	0.67	-0.86	-0.19	245	35	2005	1.02	-0.72	0.30	165	73
2006	0.64	-1.53	-0.88	285	17	2006	1.10	-1.21	-0.12	185	57
2007	0.36	-0.88	-0.52	280	22	2007	0.44	-0.73	-0.29	225	43
2008	0.83	-0.69	0.14	190	60	2008	0.80	-0.69	0.11	170	71
2009	0.51	-0.93	-0.42	255	34	2009	0.64	-0.80	-0.16	190	50
2010	0.74	-0.35	0.39	0	100	2010	0.74	-0.37	0.37	120	91
2011	0.91	-0.60	0.30	120	77	2011	1.14	-0.65	0.49	135	89
2012	0.51	-0.70	-0.18	220	42	2012	0.72	-0.57	0.16	150	79
2013	0.75	-0.59	0.16	100	80	2013	0.87	-0.52	0.35	120	92
2014	0.67	-0.26	0.41	0	100	2014	0.75	-0.16	0.59	0	100
2015	0.94	-0.37	0.57	0	100	2015	1.09	-0.35	0.75	0	100
2016	0.68	-0.38	0.29	115	84	2016	0.89	-0.36	0.53	105	96
Mean	0.66	-0.70	-0.04	174	56	Mean	0.82	-0.62	0.21	139	75
Stdev	0.16	0.32	0.41	109	31	Stdev	0.20	0.25	0.31	65	19

Table 1. Climatic mass balances (B_w-winter, B_s-summer, B_a-annual), equilibrium line altitude (ELA) and accumulation area ratio (AAR) of Hurd and Johnsons glaciers for the hydrological years 2002-2016. All of them were calculated using a specific geometry (surface elevation, glacier outlines) for each year within the study period. The last two rows include the mean and the standard deviation for each variable over the period 2002-2016.

We present in Table 2 the results of the comparison between the values calculated using a single glacier geometry for all hydrological years within our study period (the 2000 DEM, as done in Navarro et al. 2013) and those obtained using a particular geometry for each hydrological year, as described in the previous section. Only the mean and the standard deviation of the discrepancies between the results produced using both procedures is given. The complete set of results for all individual years

can be found in Recio-Blitz (2019). An important result illustrated by Table 2 is that the difference between the climatic mass balances obtained using both procedures (annually varying geometry versus single fixed glacier geometry) are not significant, in the sense that they are below the assumed error in the climatic mass balance, which rages between 0.1 and 0.2 m w.e. This is not only true for the mean values shown in Table 2, but also for the values of the individual years, as suggested by the standard deviations shown in Table 2.

Hurd Glacier						Johnsons Glacier					
Hydrol. year	ΔBw (m w.e.)	ΔBs (m w.e.)	ΔBa (m w.e.)	ΔELA (m)	ΔAAR (%)	Hydrol. year	ΔBw (m w.e.)	ΔBs (m w.e.)	ΔBa (m w.e.)	ΔELA (m)	ΔAAR (%)
Mean	0.01	-0.03	-0.02	45	-2	Mean	0.03	-0.01	0.01	-9	4
Stdev	0.03	0.07	0.06	11	5	Stdev	0.07	0.04	0.07	17	6

Table 2. Mean and standard deviation of the differences, over the period 2002-2016, between the winter (ΔBw), summer (ΔBw) and annual (ΔBa) climatic mass balances, equilibrium line altitude (ΔELA) and accumulation area ratio (ΔAAR) calculated for Hurd and Johnsons glaciers using a specific geometry (surface elevation and glacier outlines) for each year within the study period or a single glacier geometry (that of year 2000) for all years in the period.

In addition to the hypsometry of both glaciers, Fig. 2 shows a sample of the curve of annual climatic mass balance versus elevation. The figure also illustrates the procedure for graphically determining the ELA, which is the altitude where the annual balance curve intersects the zero-balance vertical straight line. An example of space distribution of the point balances b_w, b_s and b_a is presented in Fig. 3.

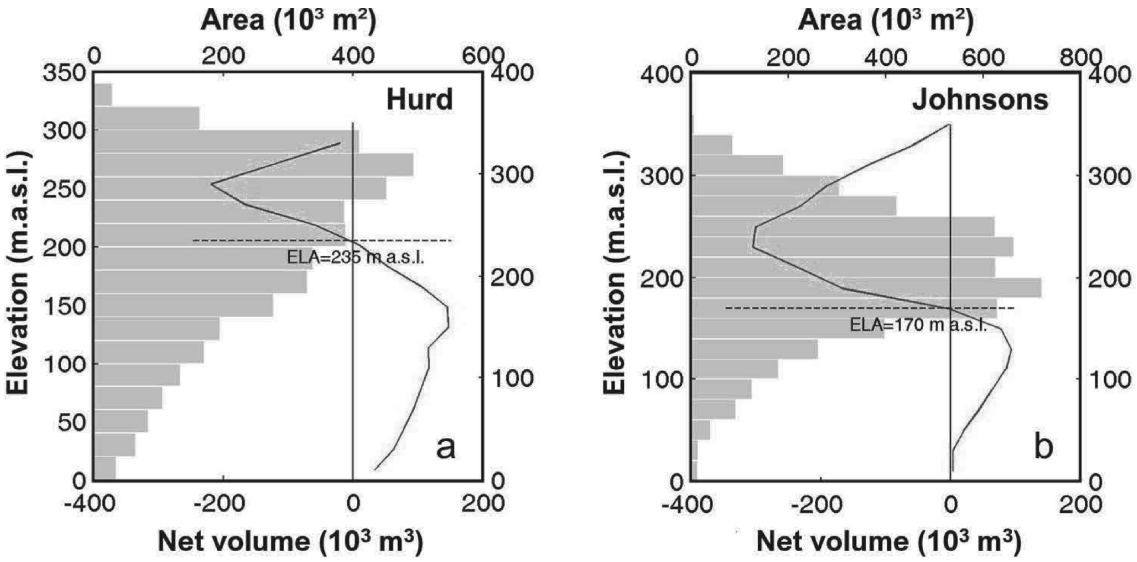

Fig. 2. Hypsometry (histogram) and sample curve of climatic mass balance versus elevation (blue line) for Hurd (a) and Johnsons (b) glaciers, for the hydrological year 2005. The black vertical straight line indicates the zero annual balance, so its intersection with the balance vs. elevation curve defines the ELA (dashed horizontal black line).

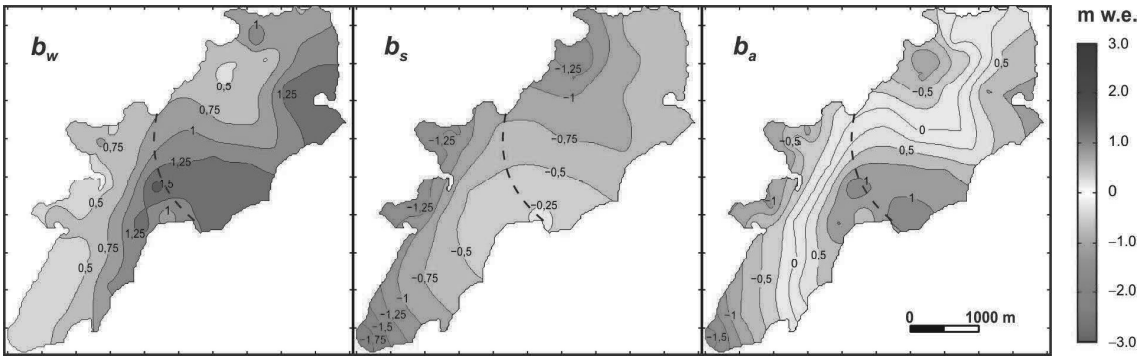

Fig. 3. An example of spatial distribution of the point climatic mass balances b_w, b_s and b_a. The example shown corresponds to the hydrological year 2005.

The temporal evolution of the glacier-wide climatic mass balances B_w, B_s and B_a, along the study period 2002–2016 is shown in Figs. 4 and 5, respectively. It can be seen a clear transition from typically negative balances (*i.e.* mass losses) at the beginning of the study period to predominantly positive balances (*i.e.* mass gains) in the second part of the study period (in particular, from hydrological year 2010).

As the entire period analysed is within the regional cooling period of the early 21st century, one could wonder why the positive CMBs did only clearly arise in the

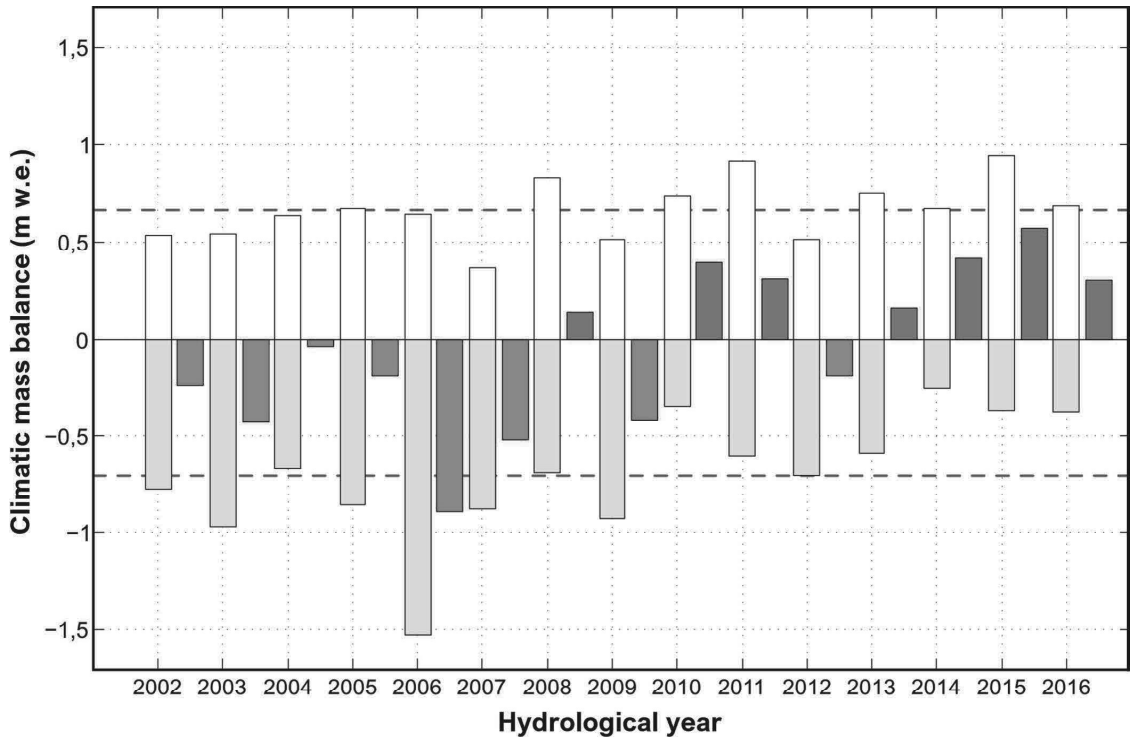

Fig. 4. Glacier-wide climatic mass balance of Hurd glacier for the hydrological years 2002-2016, calculated using the glaciological method and a specific DEM and glacier outlines for each individual year within the study period. For each year, the white bar represents the winter balance, B_w, the grey bar the summer balance, B_s, and the blue or red bar to the right of the white/grey bars the resulting annual balance, B_a, shown in blue if positive, and in red if negative. The dashed horizontal lines represent the means of the winter (positive values) and summer (negative values) balances.

second part of our study period. The reason is that, due to the intense regional warming trend occurred during the second half of the 20th century, the summer mean temperatures had reached such a high level that around a decade of subsequent cooling was needed before the glacier surface temperatures during the summer began to show widespread temperatures below the freezing point.

Figures such as 4 and 5 provide important information regarding the atmospheric conditions causing the observed annual mass balances. For instance, in Fig. 4, year 2006 had a strongly negative mass balance due to a intense summer melt (being the winter accumulation close to the mean) or, in year 2014, the annual balance was positive due to a reduced summer melt (again with an accumulation close to the mean). Or, in Fig. 4, the positive annual balances of years 2011, 2014 and 2015 had different causes, being due to an intense winter accumulation with normal summer melt (2011), a normal winter accumulation with extremely reduced summer melt (2014), or a combination of high winter accumulation and reduced summer melt (2015). Overall, the main conclusion drawn from Figs. 4 and 5 regarding the drivers of the observed mass changes is that the negative annual balances of Hurd are clearly dominated by high temperatures and associated intense summer melt, and the positive annual balances of both Hurd and Johnsons are mostly dominated by reduced summer temperatures and melt (particularly for the years 2010, 2014, 2015 and 2016), though increased accumulation also played a role.

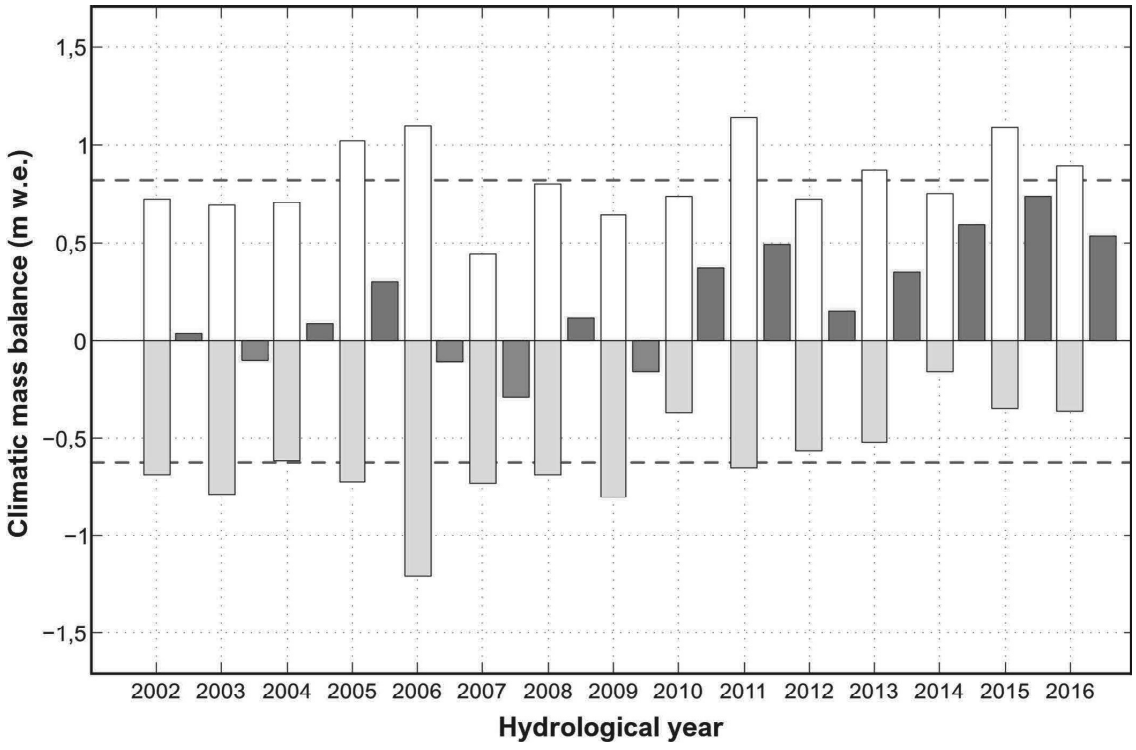

Fig. 5. Glacier-wide climatic mass balance of Johnsons glacier for the hydrological years 2002-2016, calculated using the glaciological method and a specific DEM and glacier outlines for each individual year within the study period. For each year, the white bar represents the winter balance, B_w, the grey bar the summer balance, B_s, and the blue or red bar to the right of the white/grey bars the resulting annual balance, B_a, shown in blue if positive, and in red if negative. The dashed horizontal lines represent the means of the winter (positive values) and summer (negative values) balances.

Figure 6 presents the cumulative climatic mass balance of Hurd and Johnsons glaciers, where we can observe that Hurd glacier has remained nearly in equilibrium along the study period, while Johnsons Glacier has accumulated mass on its surface along the same period. We note, however, that this comment refers to the climatic mass balance. If, as done by Navarro et al. (2013), we had added frontal ablation, mostly consisting for Johnsons Glacier of iceberg calving losses, the total mass balance of Johnsons Glacier would have remained nearly in equilibrium, as in the case of Hurd Glacier.

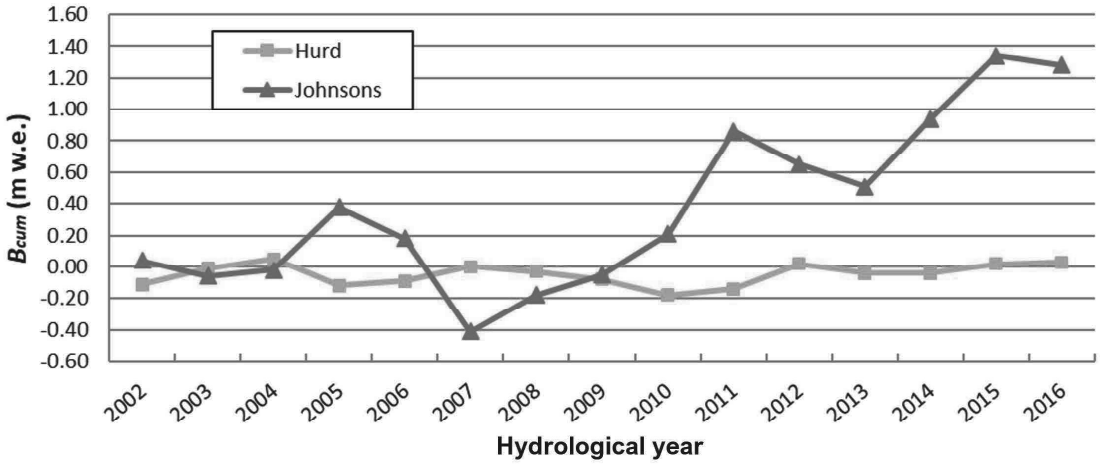

Fig. 6. Cumulative climatic mass balance of Hurd and Johnsons glaciers over the study period 2002-2016.

Figures 7, 8 and 9 illustrate the parallel evolution of the annual climatic mass balances, the ELA and the AAR (respectively) of both glaciers over the study period. As expected, when the annual balance and the AAR increase, the ELA decreases. The annual balance and the AAR of Johnsons Glacier are, for nearly every year, above those of Hurd Glacier, while the ELA shows the opposite behaviour.

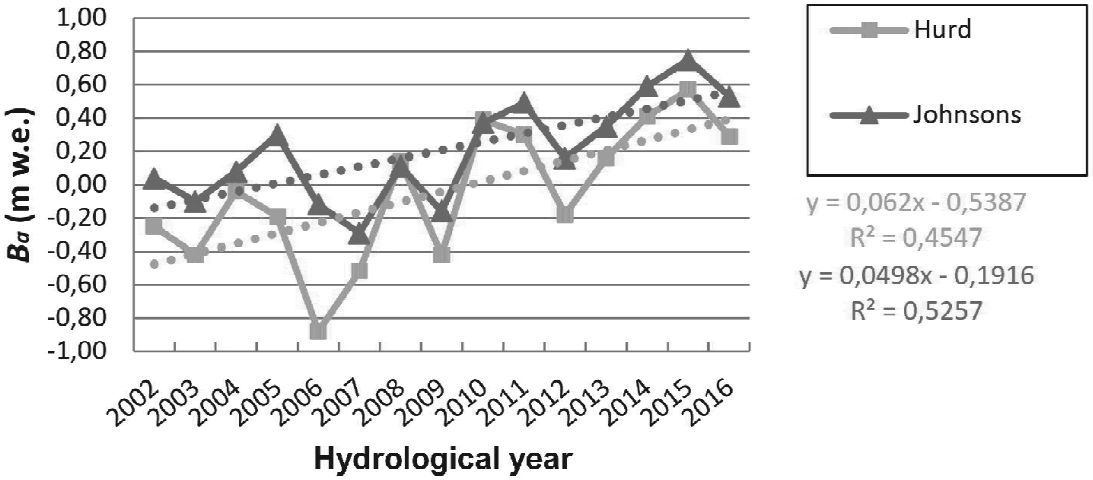

Fig. 7. Temporal evolution of the annual climatic mass balance of Hurd and Johnsons glaciers over the study period 2002-2016, together with their linear least-square fits. The p-values of the regression straight lines are 0.0058 for Hurd and 0.0022 for Johnsons.

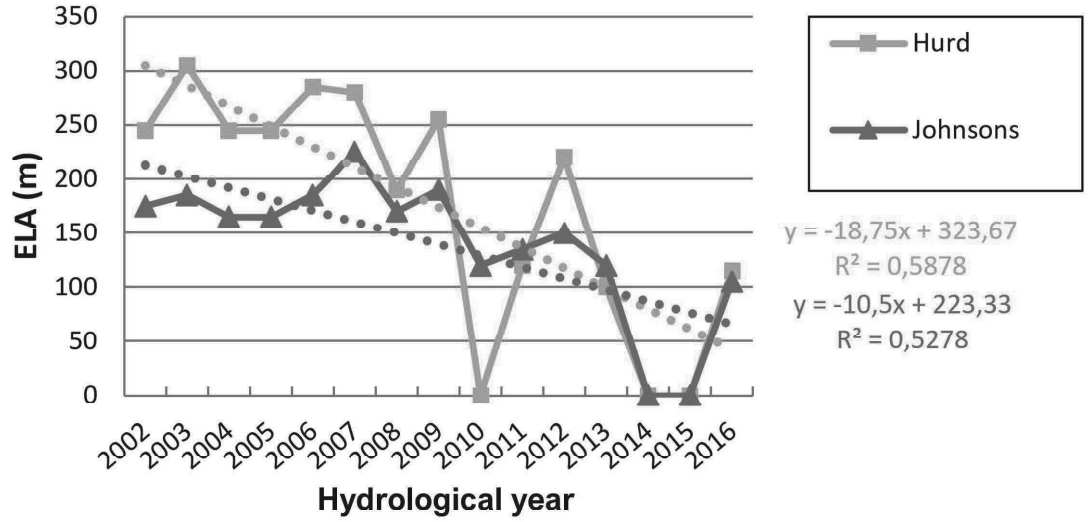

Fig. 8. Temporal evolution of the equilibrium line altitude (ELA) of Hurd and Johnsons glaciers over the study period 2002-2016, together with their linear least-square fits. The p-values of the regression straight lines are 0.0009 for Hurd and 0.0022 for Johnsons.

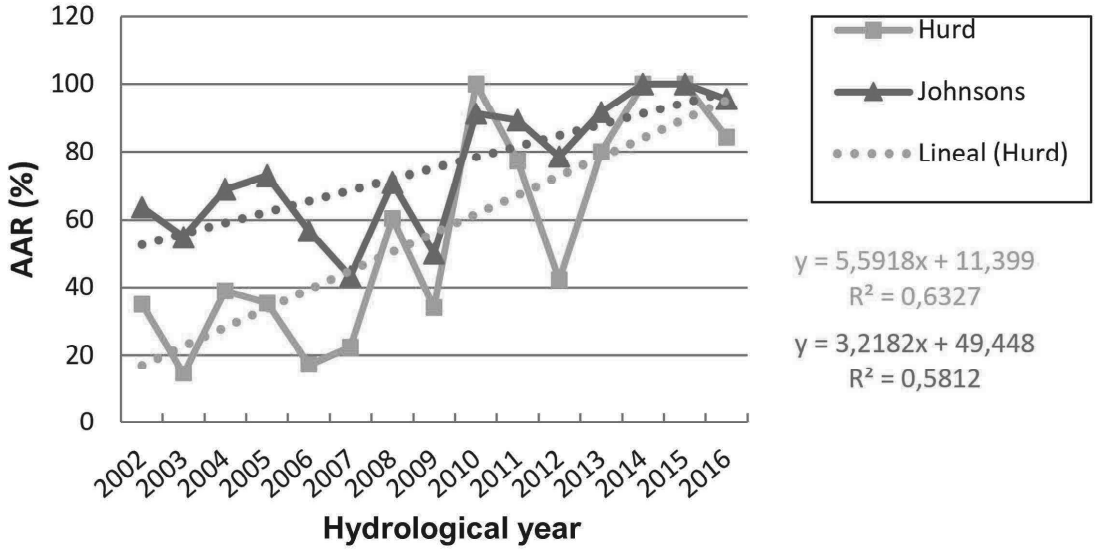

Fig. 9. Temporal evolution of the accumulation area ratio (AAR) of Hurd and Johnsons glaciers over the study period 2002-2016, together with their linear least-square fits. The p-values of the regression straight lines are 0.0004 for Hurd and 0.0010 for Johnsons.

The linear fits and their coefficients of determination R^2 shown in Figs. 7, 8 and 9, as well as the p-values included in the corresponding figure captions, indicate a clear trend to more positive mass balances, lower ELAs and larger AARs along the study period. Note that the AAR occasionally reaches 100% (and the ELA 0 m), meaning that the entire glacier surface remained snow-covered at the end of the summer; in other wors, that there was a net mass gain at every point on the glacier surface over the whole hydrological year. On the other hand, the climatic mass balances, the ELA and the AAR of both glaciers are strongly correlated, as shown by Fig. 7 and

the Pearson correlation coefficients given in Table 3. The summer balance is the parameter most strongly correlated between both glaciers. Furthermore, Table 4 illustrates the strong correlation (either positive or negative) between the various parameters for each individual glacier. For both glaciers (though more markedly for Johnsons), the (positive) correlation between the annual balance and the AAR is larger in absolute value than the (negative) correlation between the annual balance and the ELA. The (negative) correlation between ELA and AAR is larger in absolute value for Hurd than for Johnsons. The same happens with the positive correlations between the winter and annual balances, and between the summer and annual balances. This reflects the fact that Hurd is land-terminating, and less dynamic than Johnsons, and thus its climatic mass balance is more strongly governed by climate compared with the sea-terminating and more dynamic Johnsons Glacier. For the latter, factors other than climate (*e.g.*, the subglacial topography and the bathymetry of the proglacial embayment) are also expected to play a role on the mass loss mechanisms, which in this case also include processes such as iceberg calving and submarine melting at the glacier front. Finally, the fact that, for both glaciers, though more markedly for Johnsons, the correlation between summer and annual balances is larger than the correlation between winter and annual balances indicates that the interannual variability of climatic mass balance apparent in Table 1 and in Figs. 4 and 5 is governed to a larger extent by the summer balance variability.

	B_w	B_s	B_a	ELA	AAR
Hurd-Johnsons	0.77	0.98	0.90	0.88	0.92

Table 3. Pearson correlation coefficients between the time series 2002-2016 of corresponding parameters characterizing the climatic mass balance of each of the glaciers under study.

Glacier	B_a-ELA	B_a-AAR	ELA-AAR	B_w-B_a	B_s-B_a
Hurd	–0.90	0.94	–0.98	0.72	0.94
Johnsons	–0.89	0.97	–0.87	0.58	0.77

Table 4. Pearson correlation coefficients between the time series 2002-2016 of the various pairs of parameters characterizing the climatic mass balance of each individual glacier under study.

Discussion

The most immediate outcomes that can be derived from the results of our research have already been briefly discussed in the previous section. Therefore, we will focus here on discussing the evolution of the climatic mass balance of Hurd and Johnsons glacier in the context of the regional cooling period happened in the early 21st century in the northern Antarctic Peninsula and the South Shetland Islands. We will also compare the behaviour of Hurd and Johnsons mass balance records with those of similar studies at other locations in the northern AP.

Mass balance versus regional climate

We remind from the introduction that, following the long period of sustained warming of the AP region during the second half of the 20th century (Vaughan et al. 2003), a change in trend to cooling conditions happened at the turn of the century. This change in trend was perceived by Turner et al. (2016), who analysed the stacked temperature record from six coastal meteorological stations in the northern AP (north of 68 °S) since 1979 (when satellite measurements in the region became available). They detected a statistically significant change in surface air temperature trend, from a warming trend of 0.32 ± 0.20°C decade^{-1} during 1979–1997 to a cooling trend of −0.47 ± 0.25°C decade^{-1} during 1999–2014, with the change in trend happening around 1998. Turner et al (2016) attributed this change to a greater frequency of cold, east-to-southeasterly winds, resulting from more cyclonic conditions in the northern Weddell Sea linked to a strengthening of the mid-latitude jet, further amplified by the increased advection of sea ice towards the east coast of the northern AP due to the mentioned air circulation changes. Soon afterwards, Oliva et al. (2017) analysed the spatially-distributed temperature trends and the inter-decadal temperature variability from 1950 to 2015, using data from ten stations distributed across the AP region. The main result from their analysis was that the cooling period pointed out by Turner et al. (2016) mostly focused on the northernmost AP (north of 65 °S) and the SSI, where Oliva et al. (2017) reported winter (summer) temperature decreases in the order of 1.0°C (0.5°C) per decade between the decades 1996–2005 and 2006–2015. After the mid-2010s, a return to warming conditions in the region has been observed (Carrasco et al. 2021). Consequently, the 2002–2016 period covered in our analysis of CMB is nearly coincident with the coldest period in the region. This justifies the change in trend, apparent in Figs. 4 and 5, from typically negative balances (for Hurd) or close to balance (for Johnsons) at the beginning of the study period (until 2009) to predominantly positive balances (for both glaciers, though more marked for Johnsons) in the second part of the study period (from 2010). One could wonder whether a change in summer temperatures by just 0.5°C in one decade (as given by Oliva et al. 2017) is sufficient to justify such a change in the CMB in a such a short period. The answer is yes, for two reasons.

First, as pointed out by Marzeion et al. (2017), glacier mass balance (in particular, climatic mass balance) is commonly considered to be an undelayed response to atmospheric forcing; in other words, the accumulation and ablation changes resulting from atmospheric changes rapidly translate into CMB changes. This undelayed response is illustrated in Fig. 10 by the anti-correlation of summer surface temperatures at Bellinghausen station, in the neighbouring King George Island, and the summer mass balances of Hurd and Johnsons glaciers. The correlation is negative because the summer balance is negative. Bellingshausen station was selected because it has the longest temperature record in the SSI and their summer temperatures are strongly correlated with those of JCI station in Livingston Island (*e.g.* Pearson's correlation coefficient of 0.9 for the period 2005–2015; Recio-Blitz et al. 2018).

Second, and focusing now in our study region, their glaciers have been shown to be extremely sensitive to changes in air temperature. As an example, distributed temperature-radiation index melt modelling by Jonsell et al. (2012) on Johnsons Glacier showed that an increase (decrease) in mean summer surface temperature by 0.5°C implied a 56% increase (44% decrease) in surface melt.

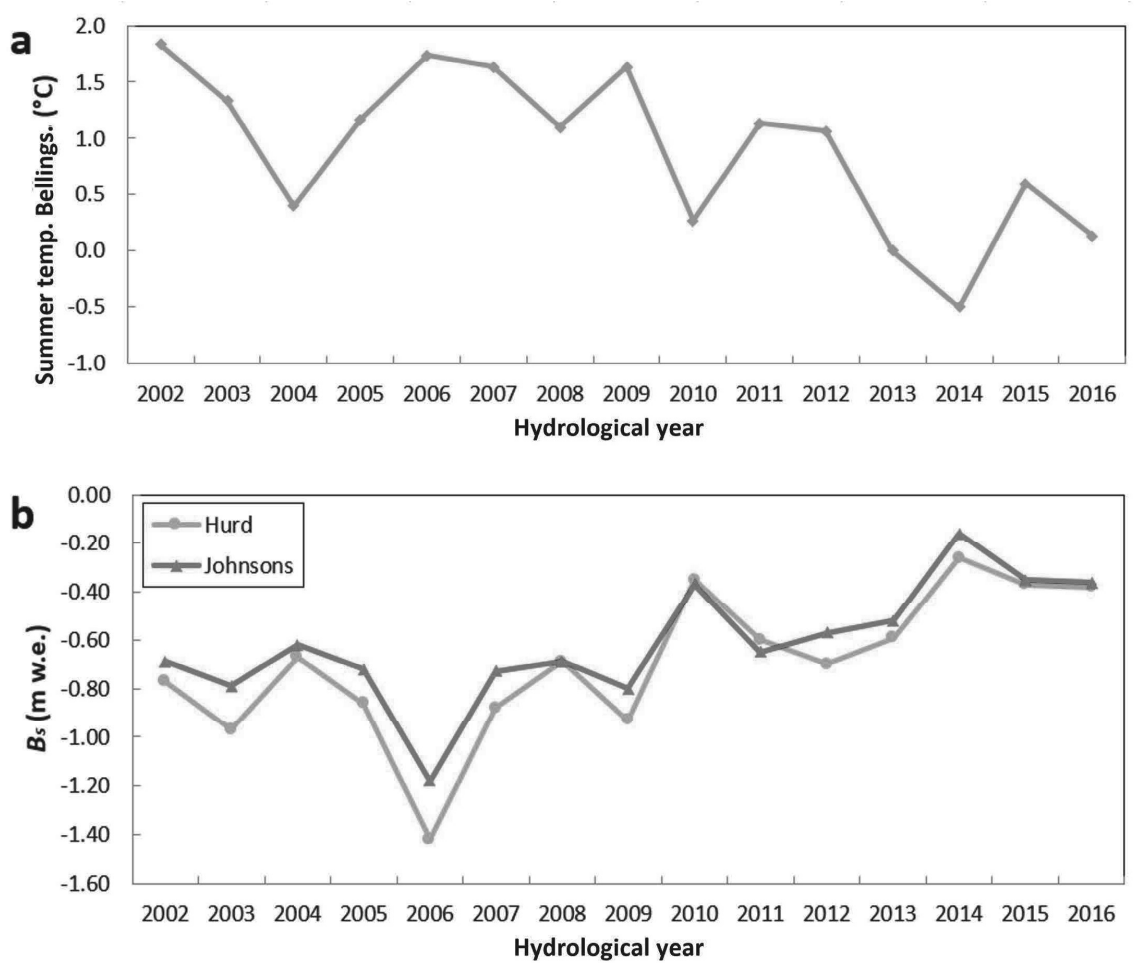

Fig. 10. a) Mean summer surface air temperature (December-January-February) at Bellingshausen Station (King George Island) over the period 2002-2016. b) Summer climatic mass balances B_s of Hurd an Johnsons glacier over the same period.

The reason for this very high sensitivity of melt to summer temperature is that most of the glacier area in the SSI is typically concentrated in the lowermost few hundred metres (see *e.g.* Shahateet et al. 2021), so the summer surface temperatures on a large fraction of the glacier area are very close to the melting point of ice. Consequently, a small temperature change results in a shift from non-melting to melting conditions or vice versa over large areas.

Finally, we note that, although the early 21st century cooling trend has been the dominant reason for the observed increases in CMB over the period 2002–2016, winter accumulation increases have also played a secondary role, as illustrated by Figs. 4 and 5 and in agreement with Navarro et al. (2013), and references therein suggesting that snow accumulation increased across the AP region over recent decades. It is also consistent with the multi-decadal increases in snowfall since the 1930s pointed out by Medley and Thomas (2019). Although these accumulation increases have occurred with longer time scales than those analysed here, they indeed contribute, together with the recent cooling period as dominant cause, to explain the decreases in CMB observed during our study period 2002–2016.

Comparison with regional glaciers

The only glacier in the northern AP region with a CMB record comparable in length (>20 yr) with those of Hurd and Johnsons glaciers is Glaciar Bahía del Diablo (63° 49' S, 57° 26' W), located on Vega Island, to the NE of the AP. It is a land-terminating glacier of ca. 14.3 km^2 in area, spanning an altitude range of 75-630 m a.s.l., and that has a NE/E orientation (Skvarca et al. 2004, Marinsek and Ermolin 2015). There are available some shorter CMB time series for other glaciers, including Bellingshausen Dome, on King George Island (hydrological years 2008–2012; Mavlyudov 2014), and Davies Dome and Whisky Glacier, on James Ross Island (hydrological years from 2009 to present, but only published 2009–2014; Engel et al. 2018). Bellingshausen Dome is situated at 62° 10' S, 58° 53' W, covers an area of about 10 km^2 and spans an altitude range of 0-250 m a.s.l. Davies Dome is located at 63° 53' S, 58° 3' W, has an area of ca. 6.5 km^2 and its altitude range is of 0-514 m a.s.l. Finally, Whisky Glacier is situated at 63° 56' S, 57° 57' W, has an area of ca. 2.4 km^2, its altitudes are within the range 215-520 m a.s.l., and presents a NNE orientation. The annual CMBs (B_a) for all of these glaciers, together with those of our study glaciers, are shown in Fig. 11.

Before comparing the mass-balance values, we note that Bahía del Diablo, Davies Dome and Whisky glaciers are measured once per year, normally in February for Bahía del Diablo (Marinsek and Ermolin 2015) and by the end of January for Davies Dome and Whisky Glacier (Engel et al. 2018). By contrast, Hurd and Johnsons, as well as Bellingshausen Dome, are/were usually measured twice per year, close to the beginning and the end of the melting season. This implies a time lag between the temporal coverage of the data reported for the SSI glaciers and those of the northern AP glaciers. This lag results in that a portion of the melt measured at a given glacier and year (approximately in March, but both February and March in the case of Davies Dome and Whisky Glacier) are attributed to the current hydrological year, for the glaciers on the SSI, but to the next hydrological year, for the glaciers on the northern AP. In fact, Engel et al. (2018) note that their CMB measurements refer to a fixed-date system that, taking year 2010 as an example, starts on 1st of February, 2009 and ends on 31st of January, 2010. Also Marinsek and Ermolín (2015) note that their measurements refer to a fixed date, though vaguely specified (~February). Actually, these are not fixed-date system measurements, as the measurement dates slightly vary from year to year due to logistic reasons, thus changing the length of the balance year. In the cases of Hurd, Johnsons and Bellingshausen Dome, the system used is a stratigraphic one, or rather a combined stratigraphic-floating date system.

The main similarity between all CMBs shown in Fig. 11 is that the negative balances tend to concentrate in the earlier years of the period (until hydrological year 2009), while the positive balances occur in the second part of the period (starting 2010). In the first part of the period there are CMB records only for Hurd, Johnsons and Bahía del Diablo (those of Bellingshausen Dome do not start until 2008). In this early period, Hurd has mass balances more negative than those of Bahía del Diablo (we compare these two glaciers because both of them are land-terminating), which we attribute to the lower altitude range of the former. There are, however, exceptions to this "rule", most markedly those of 2002 and 2008. The CMB time series of Bellingshausen Dome, limited to the period 2008–2012 (thus spanning the period of transition from negative to posi-

tive mass balances) is consistently more negative (or less positive) than those for Hurd and Johnsons glaciers (except for 2010, when they are virtually identical), in spite of their proximity. We attribute this difference to the lower altitude range of Bellingshausen Dome, which implies a larger ablation. In fact, there are available summer and winter balances for Bellingshausen Dome (Mavlyudov 2014), which show that, while the winter balances of Hurd, Johnsons and Bellingshausen Dome are very similar, the summer balances are clearly more negative for Bellingshausen Dome.

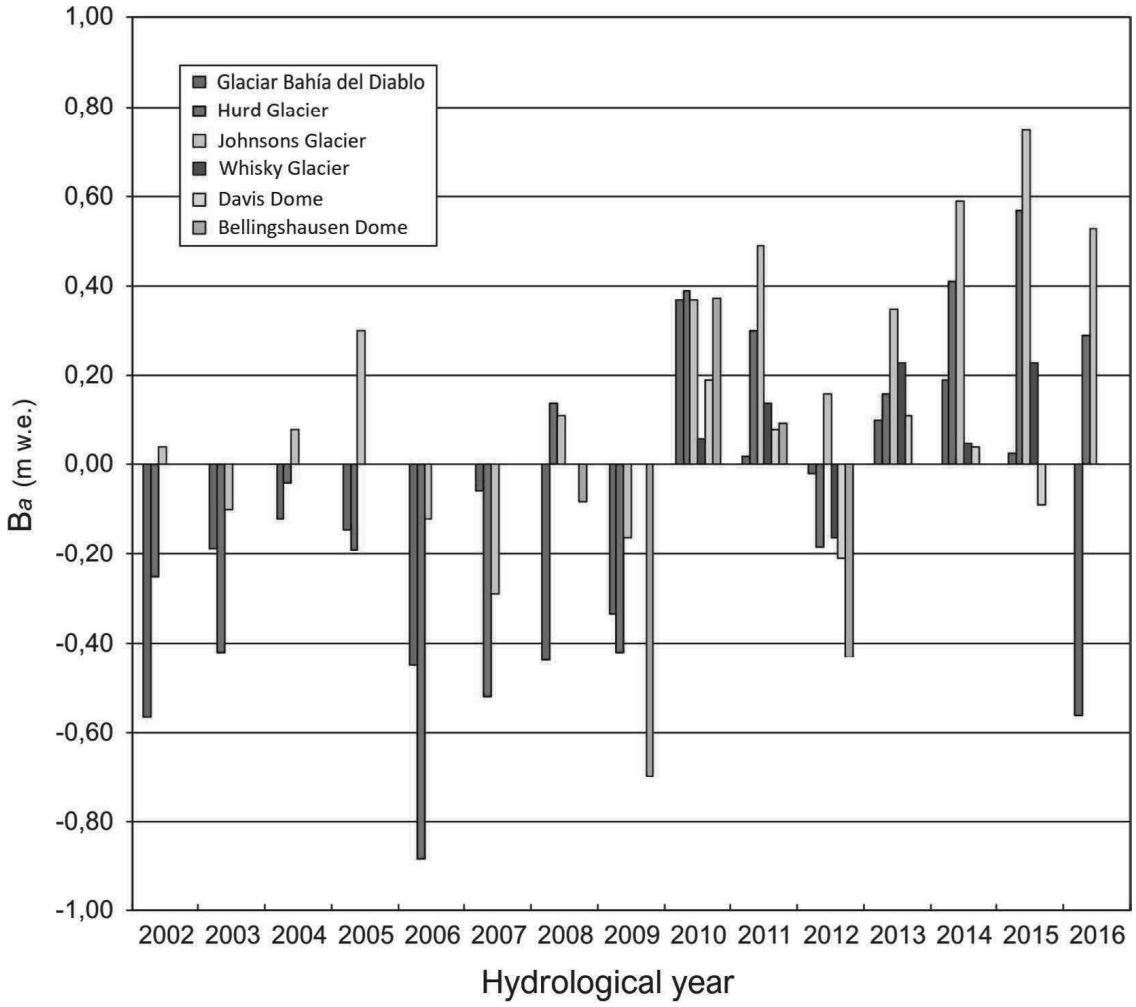

Fig. 11. Comparison of the climatic annual mass balances of various glaciers in the periphery of the northern Antarctic Peninsula. Bahía del Diablo, Hurd and Johnsons glaciers are the only ones that currently have more than 20 years of continuous mass balance records in the WGMS database for Region 19-Antarctic and Subantarctic. Glaciar Bahía del Diablo is located on Vega Island, and Davies Dome and Whisky Glacier on James Ross Island, both to the NE of the AP. Bellingshausen Dome is located on King George Island, SSI, some 100 km away from our study glaciers, Hurd and Johnsons.

Focusing now on the period dominated by positive balances (2010–2016), Hurd and Johnsons glaciers systematically show the most positive balances, more marked for Johnsons. The reasons for the more positive balance of Johnsons as compared with Hurd have already been discussed earlier. In turn, the reason why the bal-

ances for the SSI glaciers are more positive than those of the northern AP glaciers is likely the higher mean summer temperature of the SSI. As this temperature is close to melting point at the lower reaches of the glaciers, a decrease in summer temperature, even if small, implies a change from melting to non-melting conditions, resulting in more positive annual balance, as pointed out by Jonsell et al. (2012). By contrast, in the northern AP glaciers, characterised by colder summer temperatures, a minor decrease in summer temperatures does not imply a substantial change in the melting conditions. In fact, the balances of Glaciar Bahía del Diablo, Davies Dome and Whisky Glacier are, over the period of predominantly positive balances, only slightly positive (with the exception of Bahía del Diablo in 2010), in agreement with their lower mean summer temperature and their presumable lower melt. This is consistent with the melting model by Costi et al. (2018), which spans the period 1981–2014 and that predicts a substantially lower summer melt for the northern AP glaciers as compared with those in the SSI. In relation with Costi et al. (2018) modelling, we note that it predicts 2014 as the year of lowest melt, and a strongly negative melt in 2006, both in agreement with Figs. 4 and 5. We cannot evaluate other factors, such as a different accumulation regime, because Bahía del Diablo, Davies Dome and Whisky Glacir are measured only once per year, so only the annual balance can be determined, without separation of winter and summer balances. This is why Hurd and Johnsons glaciers are so valuable: in addition to the length of their time series, they provide winter and summer balances, which allows analysing the causes of the observed mass balance changes (*e.g.* if an observed change is mostly due to a change in accumulation, or in ablation, on in both).

Conclusions

The following main conclusions can be drawn from our field study and data analysis:

(1) The climatic mass balance of Hurd and Johnsons glaciers showed, over the period 2002–2016, a transition from negative or near-equilibrium values to clearly positive values, with a positive trend for the CMB of ~0.5-0.6 m w.e. decade^{-1}.

(2) In parallel, the equilibrium line altitude showed a striking negative trend of ca. –100-200 m decade^{-1}, while the accumulation area ratio increased at a rate of ~3-6% decade^{-1}.

(3) The main reason for such mass balance changes was the transient but sustained cooling period that occurred in the South Shetland Islands and the northernmost Antarctic Peninsula during the first ~15 years of the 21st century, occasionally reinforced by snow accumulation increases.

(4) The glaciers in the South Shetland Islands and the periphery of the northernmost Antarctic Peninsula have shown a similar behaviour, although the changes observed in the SSI are more marked.

(5) The use of an improved glacier geometry in the CMB calculation, with an updated DEM for each year, produced changes in the CMB below its error bars, so it did not improve noticeably the CMB results. We attribute this to the very minor changes in geometry of Hurd and Johnsons glaciers over the study period, associated to their near-equilibrium total mass balances. We speculate that, under a warming scenario, the use of an updated geometry would become relevant.

Finally, we note that, although the recent transient cooling period was accompanied by a clear decrease in the CMB, the return to regional warming conditions (Carrasco et al. 2021) is being accompanied by an associated return to negative CMBs.

References

Bañón, M., Vasallo, F. (2015): AEMET en la Antártida: Climatología y meteorología siníptica en las estaciones meteorológicas españolas en la Antártida. Madrid: AEMET, 162 p.

Carrasco, J. F., Bozkurt, D. and Cordero, R. R. (2021): A review of the observed air temperature in the Antarctic Peninsula. Did the warming trend come back after the early 21st hiatus? *Polar Science*, 28: 100653. doi: 10.1016/j.polar.2021.100653

Cogley, J. G., Hock, R., Rasmussen, L. A., Arendt, A. A., Bauder, A., Braithwaite, R. J., Jansson, P., Kaser, G., Möller, M., Nicholson, L. and Zemp, M. (2011): Glossary of glacier mass balance and related terms. UNESCO-IHP, Paris, 57(206). doi: 10.5167/uzh-53475

Costi, J., Arigony-Neto, J., Braun, M., Mavlyudov, B., Barrand, N. E., Barbosa da Silva, A., Marques, W. C. and Simões, J. (2018): Estimating surface melt and runoff on the Antarctic Peninsula using ERA-Interim reanalysis data. *Antarctic Science*, 30: 379-393. doi: 10.1017/S0954102018000391

Dyurgerov, M. (2002): Glacier mass balance and regime: data of measurements and analysis. Boulder, CO, University of Colorado. Institute of Arctic and Alpine Research. INSTAAR Occasional Paper 55, 268 p.

Edwards, T. L., *and 83 others* (2021): Projected land ice contributions to twenty-first-century sea level rise. *Nature*, 593(7857): 74-82. doi: 10.1038/s41586-021-03302-y

Engel, Z., Láska, K., Nývlt, D. and Stachoň, Z. (2018): Surface mass balance of small glaciers on James Ross Island, north-eastern Antarctic Peninsula, during 2009-2015. *Journal of Glaciology*, 64(245): 349-361. doi: 10.1017/jog.2018.17

Fox-Kemper, B., *and 17 others* (2021): Ocean, cryosphere and sea level change. *In:* V. P. Masson-Delmotte and 18 others (eds.): *Climate Change 2021: The Physical Science Basis*. Contribution of Working Group I to the Sixth Assessment Report of the Intergovernmental Panel on Climate Change, Cambridge University Press, Cambridge, United Kingdom and New York, NY, USA, pp. 1211–1362. doi: 10.1017/9781009157896.011

Hugonnet, R., *and 11 others* (2021): Accelerated global glacier mass loss in the early twenty-first century. *Nature*, 592(7856): 726-731. doi: 10.1038/s41586-021-03436-z

IPCC (2022): Summary for policymakers. *In:* H.-O. Pörtner, D. C. Roberts, M. Tignor, E. S. Poloczanska, K. Mintenbeck, A. Alegría, M. Craig, S. Langsdorf, S. Löschke, V. Möller, A. Okem and B. Rama (eds.): *Climate Change 2022: Impacts, Adaptation and Vulnerability. Contribution of Working Group II to the Sixth Assessment Report of the Intergovernmental Panel on Climate Change*, Cambridge University Press, Cambridge, UK and New York, NY, USA, pp. 3–33. doi: 10.1017/9781009325844.001

Jansson, P. (1999): Effect of uncertainties in measured variables on the calculated mass balance of Storglaciären. *Geografiska Annaler* A, 81(4): 633-642

Jonsell, U. Y., Navarro, F. J., Bañón, M., Lapazaran, J. J. and Otero, J. (2012): Sensitivity of a distributed temperature-radiation index melt model based on AWS observations and surface energy balance fluxes, Hurd Peninsula glaciers, Livingston Island, Antarctica. *The Cryosphere*, 6: 539-552. doi: 10.5194/tc-6-539-2012

Letamendia, U., Navarro, F. and Benjumea, B. (2023): Ground-penetrating radar as a tool for determining the interface between temperate and cold ice, and snow depth: A case study for Hurd-Johnsons glaciers, Livingston Island, Antarctica. *Annals of Glaciology*, 1-9. doi: 10.1017/aog.2023.73

Machío, F., Rodríguez-Cielos, R., Navarro, F., Lapazaran, J. J. and Otero, J. (2017): A 14-year dataset of in situ glacier surface velocities for a tidewater and a land-terminating glacier in Livingston Island, Antarctica. *Earth System Science Data*, 9: 751-764. doi:10.5194/essd-9-751-2017

Marinsek, S., Ermolin, E. (2015): 10 year mass balance by glaciological and geodetic methods of Glaciar Bahía del Diablo, Vega Island, Antarctic Peninsula. *Annals of Glaciology*, 56: 141-145. doi: 10.3189/2015AoG70A958

MARZEION, B., CHAMPOLLION, N., HAEBERLI, LANGLEY, W. K., LECLERCQ, P. and PAUL, F. (2017): Observation-based estimates of global glacier mass change and its contribution to sea-level change. *Surveys of Geophysics*, 38: 105-130. doi: 10.1007/s10712-016-9394-y

MAVLYUDOV, B. R. (2014): Ice mass balance of the Bellingshausen ice cap in 2007–2012 (King George Island, South Shetland Islands, Antarctica). *Led I Sneg* [*Ice and Snow*], 1: 27-34. [In Russian with English summary]

MEDLEY, B., THOMAS, E. R. (2019): Increased snowfall over the Antarctic Ice Sheet mitigated twentieth-century sea-level rise. *Nature Climate Change*, 9(1): 34-39. doi: 10.1038/s41558-018-0356-x

MENSAH, D., LAPAZARAN, J. J., OTERO, J. and RECIO-BLITZ, C. (2022): A restitution method to reconstruct the 2001–13 surface evolution of Hurd Glacier, Livingston Island, Antarctica, using surface mass balance data. *Journal of Glaciology*, 68(269): 443-456. doi: 10.1017/jog.2021.104

MOLINA, C., NAVARRO, F. J., CALVET, J., GARCÍA-SELLÉS, D. and LAPAZARAN, J. J. (2007): Hurd Peninsula glaciers, Livingston Island, Antarctica, as indicators of regional warming: ice-volume changes during the period 1956-2000. *Annals of Glaciology*, 46: 43-49. doi: 10.3189/172756407782871765

NAVARRO, F. J. (2021): Sea-level rise. Which is the role of glaciers and polar ice sheets? *Mètode Science Studies Journal*, 11: 173-181. doi: 10.7203/metode.11.16988

NAVARRO, F. J., OTERO, J., MACHERET, YU. YA., VASILENKO, E. V., LAPAZARAN, J. J., AHLSTRØM, A. P. and MACHÍO, F. (2009): Radioglaciological studies on Hurd Peninsula glaciers, Livingston Island, Antarctica. *Annals of Glaciology*, 50(51): 17-24. doi: 10.3189/172756409789097603

NAVARRO, F. J., JONSELL, U. Y., CORCUERA, M. I. and MARTÍN-ESPAÑOL, A. (2013): Decelerated mass loss of Hurd and Johnsons glaciers, Livingston Island, Antarctic Peninsula. *Journal of Glaciology*, 59(214): 115-128. doi: 10.3189/2013JoG12J144

OLIVA, M., NAVARRO, F., HRBÁČEK, F., HERNÁNDEZ, A., NÝVLT, D., PEREIRA, P., RUIZ-FERNÁNDEZ, J. and TRIGO, R. (2017): Recent regional cooling of the Antarctic Peninsula and its impacts on the cryosphere. *Science of the Total Environment*, 580: 210-223. doi: 10.1016/j.scitotenv.2016.12.030

OTERO, J., NAVARRO, F. J., MARTIN, C., CUADRADO, M. L. and CORCUERA, M. I. (2010): A three-dimensional calving model: Numerical experiments on Johnsons Glacier, Livingston Island, Antarctica. *Journal of Glaciology*, 56(196): 200-214. doi: 10.3189/002214310791968539

PFEFFER, W. T. *and 18 others*, and the RANDOLPH CONSORTIUM (2014): The Randolph Glacier Inventory: A globally complete inventory of glaciers. *Journal of Glaciology*, 60(221): 537-552. doi: 10.3189/2014JoG13J176

RECIO-BLITZ, C. (2019): Balance de masa reciente y dinámica de los glaciares de la Península Hurd (Isla Livingston, Antártida) en un contexto de clima cambiante. PhD thesis, Universidad Politécnica de Madrid, 234 p.

RECIO-BLITZ, C., NAVARRO, F. J., OTERO, J., LAPAZARAN, J. and GONZÁLEZ, S. (2018): Effects of recent cooling in the Antarctic Peninsula on snow density and surface mass balance. *Polish Polar Research*, 39(4): 457-480. doi:10.24425/118756

RIZZOLI, P., *and 10 others* (2017): Generation and performance assessment of the global TanDEM-X digital elevation model. *ISPRS Journal of Photogrammetry and Remote Sensing*, 132: 119-139. doi:10.1016/j.isprsjprs.2017.08.008

RODRÍGUEZ-CIELOS, R. (2014): Integración de modelos numéricos de glaciares y procesado de datos de georradar en un sistema de información geográfica. PhD Thesis, Universidad Politécnica de Madrid, 341 p.

RODRÍGUEZ-CIELOS, R., AGUIRRE DE MATA, J., DÍEZ GALILEA, A., ÁLVAREZ ALONSO, M., RODRÍGUEZ CIELOS, P. and NAVARRO VALERO, F. (2016): Geomatic methods applied to the study of the front position changes of Johnsons and Hurd glaciers, Livingston Island, Antarctica, between 1957 and 2013. *Earth System Science Data*, 8: 341-353. doi: 10.5194/essd-8-341-2016

SHAHATEET, K., SEEHAUS, T., NAVARRO, F., SOMMER, C. and BRAUN, M. (2021): Geodetic mass balance of the South Shetland Islands Ice Caps, Antarctica, from differencing TanDEM-X DEMs. *Remote Sensing*, 13(17): 3408. doi: 10.3390/rs1317340

SKVARCA, P., DE ANGELIS, H. and ERMOLIN, E. (2004): Mass balance of 'Glaciar Bahía del Diablo', Vega Island, Antarctic Peninsula. *Annals of Glaciology*, 39: 209-213. doi: 10.3189/172756404781814672

SUGIYAMA, S., NAVARRO, F. J., SAWAGAKI, T., MINOWA, M., SEGAWA, T., ONUMA, Y., OTERO, J. and VASILENKO, E. V. (2019): Subglacial water pressure and ice-speed variations at Johnsons Glacier, Livingston Island, Antarctic Peninsula. *Journal of Glaciology*, 65(252): 689-699. doi: 10.1017/jog.2019.45

TURNER, J., LU, H., WHITE, I., KING, J. C., PHILLIPS, T., HOSKING, J. S., BRACEGIRDLE, T. J., MARSHALL, G. J., MULVANEY, R. and DEB, P. (2016): Absence of 21st century warming on Antarctic Peninsula consistent with natural variability. *Nature*, 535(7612): 411-415. doi: 10.1038/nature18645

VAUGHAN, D. G., MARSHALL, G., CONNOLLEY, W., PARKINSON, C., MULVANEY, R., HODGSON, D., KING, J., PUDSEY, C. and TURNER, J. (2003): Recent rapid regional climate warming on the Antarctic Peninsula. *Climatic Change*, 60: 243-274. doi: 10.1023/A:1026021217991

WESSEL, B., HUBER, M., WOHLFART, C., MARSCHALK, U., KOSMANN, D. and ROTH, A. (2018): Accuracy assessment of the global TanDEM-X Digital Elevation Model with GPS data. *ISPRS Journal of Photogrammetry and Remote Sensing*, 139, 171-182. doi:10.1016/j.isprsjprs.2018.02.017

ZEMP, M., *and 16 others* (2019): Global glacier mass changes and their contributions to sea-level rise from 1961 to 2016. *Nature*, 568(7752): 382-86. doi: 10.1038/s41586-019-1071-0

Web sources / Other sources

[1] https://www.gtn-g.ch/data_catalogue_glacreg/ (accessed 16/12/2023). doi: 10.5904/gtng-glacreg-2017-07
[2] https://wgms.ch/ (accessed 16/12/2023)
[3] https://science.nasa.gov/resource/asters-global-digital-elevation-model/ (accessed 16/12/2023)
[4] https://saga-gis.sourceforge.io/en/index.html (accessed 16/12/2023)
[5] https://grass.osgeo.org/ (accessed 16/12/2023)